Received: 5 September 2018 | Revised: 1 November 2018 | Accepted: 4 November 2018
DOI: 10.1002/ardp.201800266

FULL PAPER

DPhG ARCH PHARM
Archiv der Pharmazie

Semi-synthesis, antibacterial activity, and molecular docking study of novel pleuromutilin derivatives bearing cinnamic acids moieties

Yu Deng[1] | Da Tang[1] | Qiu-ru Wang[2] | Sheng Huang[1] | Li-zhi Fu[1] | Cheng-hong Li[1]

[1] Institute of Veterinary Sciences and Pharmaceuticals, Chongqing Academy of Animal Sciences, Rongchang, China

[2] West China School of Medicine, Sichuan University, Chengdu, China

Correspondence
Cheng-hong Li, Institute of Veterinary Sciences and Pharmaceuticals, Chongqing Academy of Animal Sciences, Rongchang 402460, China.
Email: lchong_cqaa@hotmail.com

Funding information
Chongqing Basic Scientific Research Project, Grant number: 16438; Chongqing Agricultural Development Fund, Grant number: 17412

Abstract

To develop new antibiotics owning a special mechanism, we used the molecular assembly method to synthesize a series of novel pleuromutilin derivatives containing a cinnamic acid scaffold at the C-14 side chain. We evaluated their antibacterial activity and used *in silico* molecular docking to study their binding mode with the target. The structure–activity relationship (SAR) study suggested that compounds with NO_2 (**13e**), OH (**13u**), and NH_2 (**13y**) appeared more active (0.0625–2 μg/mL) *in vitro* against several penicillin-resistant Gram-positive bacteria and the position of the substituent on the benzene ring would affect the activity. The *in vivo* efficacy investigation of **13e**, **13u**, and **13y** with once daily intragastric (i.g.) administration at 40 mg/kg for 3 consecutive days in a mouse systemic infection model showed that **13u** had equal activity as valnemulin providing the mice with 60% survival, while **13e** and **13y** gave 30 and 40% survival, respectively. The molecular docking studies indicated that π–π stacking and hydrogen bond formation played important roles in improving the antibacterial activity.

KEYWORDS
antibiotics, cinnamic acid, molecular assembly, pleuromutilin, structure–activity relationship

1 | INTRODUCTION

The dramatic increasing appearance of multidrug-resistant bacteria has threatened the public health in the whole world.[1] Among these multidrug-resistant Gram-positive bacteria, methicillin-resistant *Staphylococcus aureus* (MRSA), penicillin-resistant *Streptococcus pneumoniae* (PRSP), and vancomycin-resistant enterococci (VRE) are the major control objectives. The grim situation has caused people's high vigilance and concern, which prompts scientists to develop new antibiotics with novel mechanisms of action and minimal cross-resistance. For example, the members of Mur ligase family MurC to MurF that are involved in the intracellular biosynthesis stage of bacterial peptidoglycans, have emerged as attractive targets for antibiotics design and some progress has been achieved.[2,3] A recent research reported two synthetic retinoid antibiotics discovered through high-throughput screening displayed excellent activity against Gram-positive bacteria by disrupting cell lipid bilayers.[4] All of these urged us to focus on some effective molecules to develop new antibacterial agents, for instance, pleuromutilin.

Pleuromutilin **1** (Figure 1) is a natural product with moderate antibacterial activity first isolated from the fungi *Pleurotusmutilus* (now

Yu Deng and Da Tang contributed equally to this work.

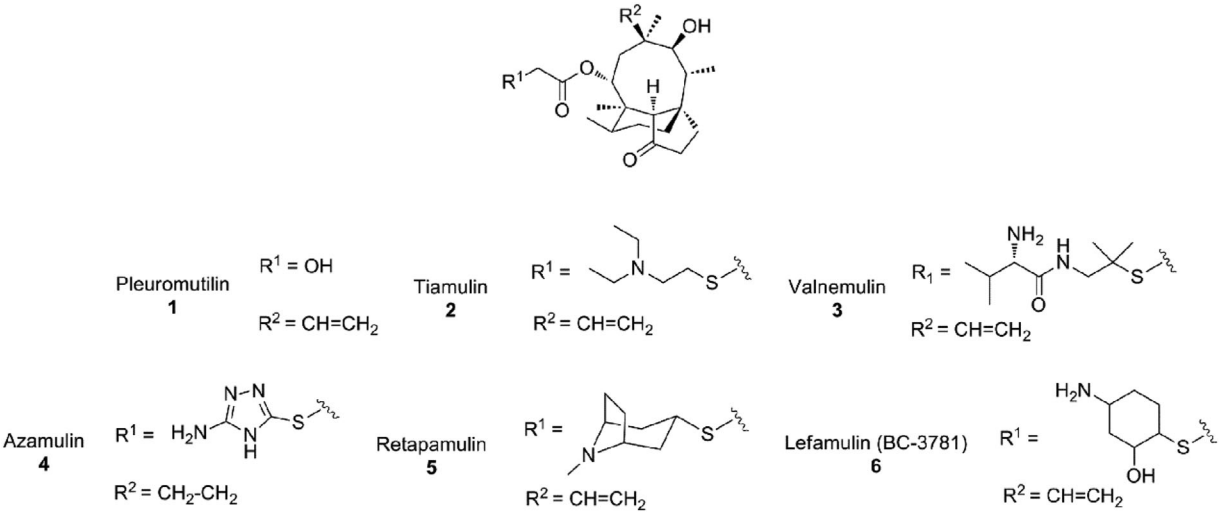

FIGURE 1 The structures of pleuromutilin and related drugs

called *Clitopilusscyphoides*).[5] The mechanism studies have confirmed that pleuromutilin derivatives selectively target bacterial 50S ribosome subunit and display no cross-resistance with antibiotics in clinical utilization.[6–8] Since its unique action mode, pleuromutilin has attracted growing attention in the development of novel antibacterial agents for the therapy of multi-drug resistant bacterial infections.[9] These researches resulted in the discovery of tiamulin **2** and valnemulin **3**[10] which were approved as veterinary medicines in 1979 and 1999, respectively. Further studies led to the development of azamulin **4** which aimed at human use. However, the phase I clinical studies showed that the azamulin has poor bioavailability and serious CYP450 inhibition.[11] Subsequently, retapamulin **5** was initiated by GlaxoSmithKline and approved for treating human skin infections and soft tissues infection in 2007, but low clinical efficacy was also observed in the treatment of patients with secondarily infected open wound (SIOW) infections caused by MRSA.[12] Recently, Nabriva Therapeutics reported their efforts in developing lefamulin (BC-3781) **6** as the first pleuromutilin analogue for the treatment of systemic bacterial skin infections.[13] At present, this compound has gone to the stage of community-acquired bacterial pneumonia phase III clinical and acute bacterial skin and skin structure infections (ABSSSI) phase II clinical trials.[14,15]

However, a fact that should be acknowledged that like almost all classes of antibiotics, pleuromutilin derivatives were smoothly used as veterinary medicine while the progress of human use was very limited. The main reason is probably the features of pleuromutilin, such as metabolic instability, lack of oral bioavailability, hepatotoxicity would make the side-chain chemistry of it become challenging. Despite a large number of synthetic pleuromutilin derivatives including marketed drugs either for human or veterinary use, usually contain thioether-type in the C14 side chain, other pleuromutilin compounds with superior skeleton and groups in the side chain have been rarely synthesized and evaluated their activity. To our knowledge, piperazine ring is one of the 25 most common nitrogen heterocycles in approved marketed drugs by the US FDA. From the perspective of pharmaceutical chemistry design, this ring not only has a good three-dimensional structure, but also compounds with this structure usually have excellent pharmacokinetic property and can increase the water solubility and metabolic stability of the compounds. In addition, several approved drugs like aripiprazole **7**,[16] ketoconazole **8**,[17] and levofloxacin **9**[18] (Figure 2) containing piperazine structure encouraged us to link piperazine ring to the side chain of pleuromutilin. Furtherly, cinnamic acid derivatives have been verified to own a wide variety of biological activities such as antimicrobial,[19] antimycobacterium,[20] anti-cell proliferative,[21] etc. Moreover, piperazine ferulate **10**, a kind of non-peptide endothelin receptor antagonists approved by CFDA, has good therapeutic effect on kidney diseases.[22] Based on these points, our study aimed to introduce piperazine ring at the C22 of

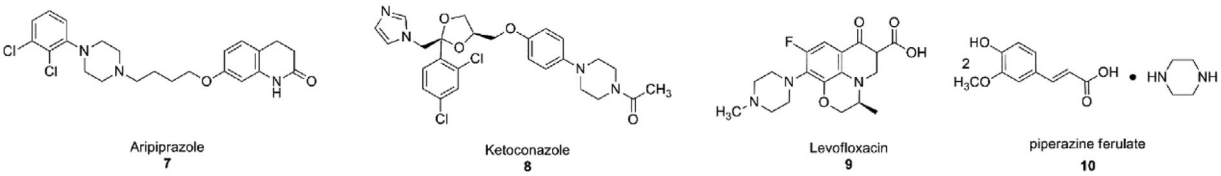

FIGURE 2 Approved drugs containing piperazine

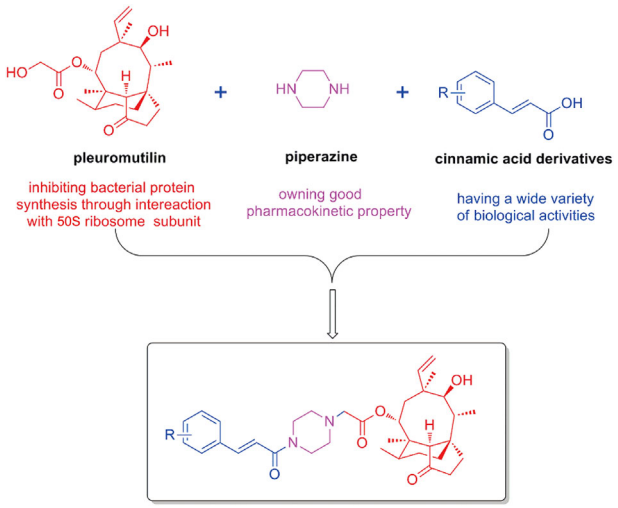

FIGURE 3 Design scheme of target compounds

pleuromutilin as a linker and integrate cinnamic acid derivatives and pleuromutilin to form hybrids (Figure 3) to investigate the anti-bacterial activity of pleuromutilin derivatives.

2 | RESULTS AND DISCUSSION

2.1 | Synthesis

The synthesis of our target compounds is showed in Scheme 1. The commercial available pleuromutilin **1** was reacted with *p*-toluene sulfonylchloride (TsCl) using NaOH as the base to give 14-O-(*p*-toluenesulfonyloxyacetyl) mutilin **10**. Then compound **10** was reacted with 1-boc-piperazine in the presence of K_2CO_3 and 2 mol% NaI in acetonitrile. The obtained crude product was treated with 6 N HCl in 1,4-dioxane at room temperature overnight to give compound **11**. Next, HATU was employed to promote the condensation of the resulting salt **11** with cinnamic acid derivatives in DMF to yield **13a–d** and **13f–x**. The messy and low yield of the condensation of 2-nitrocinnamic acid (**12e**) and 4-aminocinnamic acid (**12y**) with **11** urged us to choose another route. The reduction of compound **12q** using Fe powder and HCOOH gave compound **12y** in 26% yield. **12e** and **12y** were condensed with 1-boc-piperazine followed by deprotection with 6 N HCl in 1,4-dioxane to provide **15e** and **15y** in 76.5 and 61.2% yield for two steps, respectively. The hybridization of **15e** and **15y** with compound **10** offered **13e** and **13y**.

2.2 | *In vitro* antibacterial activity assay

The pathogens inhibition assay was performed to evaluate the *in vitro* anti-bacterial activity of all prepared compounds employing valnemulin as the positive control. The minimum concentration (MIC) values were revealed as the range of three different clinical isolates for each bacterium.

Pleuromutilin/cinnamic acid hybrids containing both electron withdrawing and donating groups were introduced to explore the SAR, as shown in Table 1. The MICs data showed that compounds bearing electron-donating groups, e.g., 4-CH_3 (**13r**) or 4-OCH_3 (**13s**), displayed similar potency to compound **13a** that was more effective against methicillin sensitive bacteria than against methicillin-resistant pathogen. The presence of 4-OH in **13u** and 4-NH_2 in **13y** substantially increased *in vitro* activity against all strains compared with that of **13r** and **13s** and even showed superior to that of valnemulin. The 4-Cl and 4-Br substituted derivatives, namely **13c** and **13d**, were slightly more active than **13a** but not as good as **13n** (4-F) whose MICs ranged from 0.125 to 1 μg/mL. Surprisingly, **13q** with strong electron-withdrawing group 4-NO_2 presented enhanced anti-bacterial activity compared to

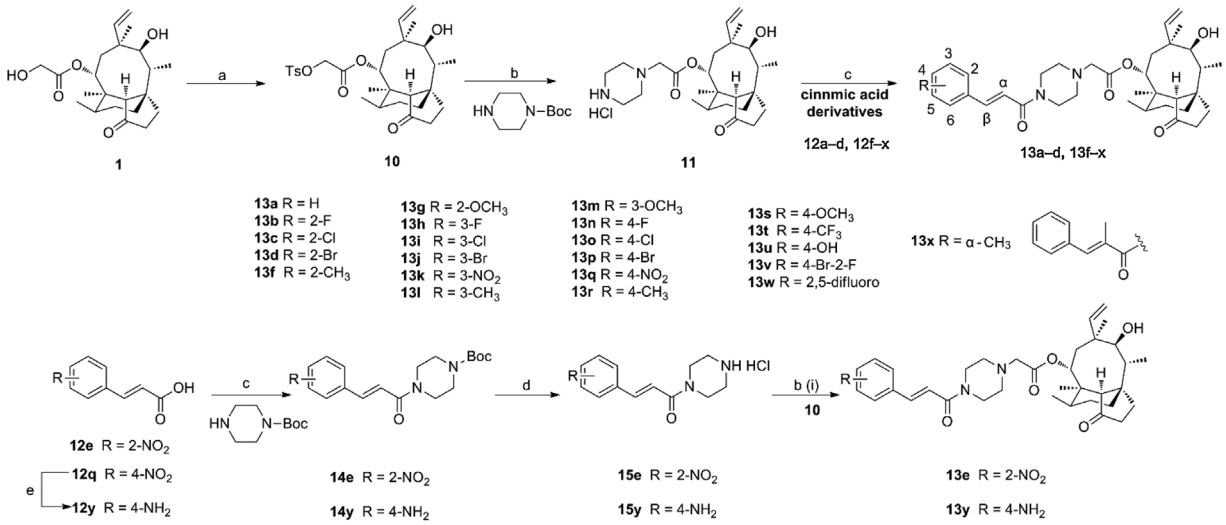

SCHEME 1 The synthesis of target compounds **13a–y**. Reagents and conditions: (a) TsCl, NaOH, H_2O, *t*-butyl methyl ether, reflux, 1 h; (b) (i) K_2CO_3, 2 mol% NaI, CH_3CN, 85°C, 4 h; (ii) HCl/1,4-dioxane, rt, 2 h; (c) HATU, Et_3N, DMF, rt, 3 h. (d) HCl/1,4-dioxane, 45°C, overnight; (e) Fe/HCOOH, 60°C, overnight

TABLE 1 Antibacterial activity (MIC, μg/mL) of pleuromutilin derivatives containing cinnamic acid *in vitro*

	MIC[a] (μg/mL)						
Compound	MSSA[b]	MRSA[b]	MSSE[b]	MRSE[b]	PSSP[b]	PRSP[b]	*E. coli*
13a	0.5–1	2–4	0.25–2	4	1–2	4	64
13b	0.25	0.25–0.5	0.5	1–2	0.5	1–4	>64
13c	0.5	0.5–1	0.5	1	1-2	2–4	>64
13d	0.5	1–2	0.5–1	0.5–1	0.5	1	>64
13e	0.0625	0.0625–0.25	0.125–0.5	0.25	0.25–1	0.25–1	64
13f	1–2	2	1–2	2	1–4	2	32
13g	0.125	0.25–0.5	0.25–0.5	0.25–1	0.5–1	1–2	64
13h	0.5–1	0.5–1	1	1–2	1–2	4	64
13i	0.5	0.5–1	1–2	2	1	2	64
13j	0.5	1	0.5	1	1	2	64
13k	0.25–1	0.5-2	0.25	1	0.5–1	2	32
13l	0.125–0.5	0.5–1	0.5	1–2	0.5	1–2	32
13m	0.125–0.25	0.25	0.125–0.5	0.5	0.5–1	0.5–1	32
13n	0.25	0.25–0.5	0.5	0.5–1	0.5	1	>64
13o	0.25–0.5	0.5–2	0.5–1	1	0.5	1–2	32
13p	0.5–1	1–2	0.5	0.5–1	0.5	1–2	32
13q	0.0625	0.125–1	0.125	0.5	0.5–1	0.5–1	32
13r	1–2	1–4	0.5–2	4	0.5	2	64
13s	2	2–4	1	2	1	1	64
13t	0.5	1–2	1	1–2	0.5	1–4	32
13u	0.0625	0.125	0.125	0.25–0.5	0.25–1	0.25–2	16
13v	0.25–0.5	0.25–1	0.5	0.5–2	1	2–8	64
13w	0.125–1	0.5–1	0.25–0.5	0.25–2	1–2	2	64
13x	1–2	1–4	0.5–2	2–4	0.25–2	4	32
13y	0.0625–0.125	0.0625–1	0.0625–0.125	0.0625–1	0.25–0.5	0.25–1	32
Valnemulin	0.0625	0.25–0.5	0.125–0.5	0.5–2	0.25–1	0.5–1	16

[a]Abbreviations are as follows: MIC, minimum inhibitory concentration; MSSA, methicillin-sensitive *Staphylococcus aureus*, three strains; MRSA, methicillin-resistant *Staphylococcus aureus*, three strains; MSSE, methicillin-sensitive *Staphylococcus epidermidis*, three strains; MRSE, methicillin-resistant *Staphylococcus epidermidis*, three strains; PSSP, methicillin-sensitive *Streptococcus pneumoniae*, three strains; PRSP, penicillin-resistant *Streptococcus pneumoniae*, three strains; *E.coli*, *Escherichia coli*.

[b]MIC values are obtained as the range of different strains of the same type. Single number represents the same MIC value for three different strains. Each strain was repeated three times. All of the strains were isolated from the clinical bacteria in Chongqing Daping Hospital and reserved in Veterinary & Veterinary Drug Research Institute, Chongqing Academy of Animal Sciences.

13n except for PSSP and PRSP, whereas the activity of the 4-CF_3 substituted derivative **13t** was lower than other 4-substituted cinnamic acid derivatives embodying electron-withdrawing groups.

Identical trends were observed in 2-substituted cinnamic acid derivatives. **13e** with 2-NO_2 presented the most strong potency against MSSA, MRSA, MSSE, and MRSE, which showed two- to eightfold higher activity than its 3-position regioisomer **13k**. Compounds bearing electron-withdrawing groups like **13b** (2-F), **13c** (2-Cl), and **13d** (2-Br) showed improved anti-bacterial activities in comparison with **13f** owning 2-CH_3 but were less effective than **13g** possessing 2-OCH_3.

The investigation of 3-substituted cinnamic acid derivatives gave different trends compared to other two kinds of substituted derivatives. The electron-donating groups substituted compounds such as **13l** (3-CH_3) and **13m** (3-OCH_3), inhibited the growth of tested bacteria more effectively than those compounds with halogen (**13h–13j**) as well as nitro (**13k**). The results indicate that the position of substituent had a notable effluence on the activity.

The inspection of compounds **13v** and **13w** against the listed strains showed that MICs of multi-halogen substitutions were equal or close to that of single-halogen substitution (**13v** vs. **13b** and **13p**, **13w** vs. **13b** and **13h**). **13x** bearing a CH_3 substituent in the α-position of cinnamic acid lowered a bit of activity compared to **13a**.

The antibacterial activity against Gram-negative bacterium of **13a–y** were also tested. **13u** and valnemulin possessed the same

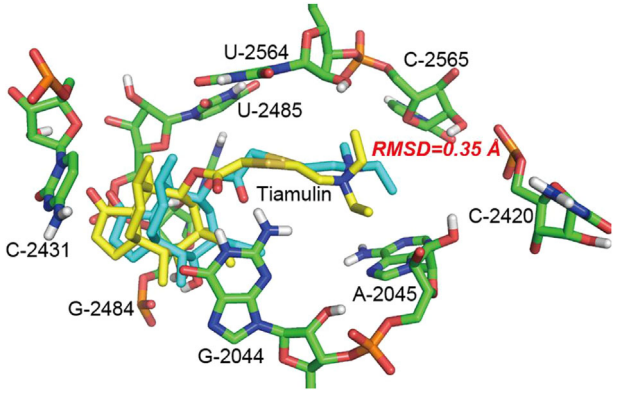

FIGURE 4 Docking mode of tiamulin in the active site of 50s ribosome subunit: blue indicates the conformation of tiamulin in the crystal structure; yellow indicates the conformation after redock; green indicates surrounded residue

moderate potency against *Escherichia coli* (MIC = 16 μg/mL) while MIC values of other compounds were more than 32 μg/mL. The testing result showed that none of this class of compounds were effective against *E. coli*, which were consistent with other pleuromutilin derivatives.

2.3 | *In silico* molecular docking

Since their excellent anti-bacterial activity, compounds **13e**, **13u**, **13y** and valnemulin were selected to study molecular docking. The X-ray structure of ribosome-tiamulin (PDB 1D: 1XBP) was employed to construct the initial model (Figure 4). The docking method was validated by the redock of tiamulin, with the root mean square deviations (RMSD) of tiamulin in crystal structure relative to tiamulin in the redock model being 0.35 Å, which confirmed the approach was appropriate.

Specifically, **13e** and **13u** displayed the same interaction mode. As shown in Figures 5 and 6, **13e** and **13u** were found to form two strong hydrogen bonds with 50S ribosome. The interaction between the OH on C-11 and the phosphate of G2484 formed one hydrogen bond and the oxygen atom of carbonyl on C-21 interacted with residue G2044 exhibited another hydrogen bond. It was also found that the NO_2 of **13e** and the benzene ring of **13u** had a π–π stacking with residue A2045, respectively. The calculation showed that the binding energy of **13e** with ribosome was −7.09 kcal/mol while that of **13u** reduced to −7.19 kcal/mol.

The molecular docking of **13y** bearing 4-NH_2 displayed five hydrogen bonds (Figure 7). Three hydrogen bonds were formed by the interaction between OH and residue G2484 as well as carbonyl on C-21 and residue G2044. The NH_2 on the benzene ring formed other two hydrogen bonds with the phosphate of C2420. The binding energy of **13y** was −7.57 kcal/mol and lower than that of both **13e** and **13u**. The docking result may explain why **13y** exhibited better *in vitro* antibacterial activity and suggested that the introduction of NH_2 to the C14 side chain would be an effective tactic for the design of pleuromutilin derivatives.

The docking research of the positive control compound valnemulin was also made to compare its binding mode with that of above docking compounds. The result showed valnemulin formed four hydrogen bonds with the 50S ribosome subunit and rendered a similar docking mode to that of **13y** in general (Figure 8). The main difference was that the amide of valnemulin formed one hydrogen bond with C2046 residue and another hydrogen bond interaction was found between the NH_2 and U2564 residue. The calculated binding free energy of valnemulin was −7.94 kcal/mol, being lower than that of **13e**, **13u**, and **13y**. However, the *in vitro* antibacterial activity of valnemulin was equal or even lower than that of these three compounds.

2.4 | *In vivo* efficacy of compounds 13e, 13u, and 13y

Due to their excellent activity *in vitro* against MRSA, the investigation of the *in vivo* efficacy of compounds **13e**, **13u**, and **13y** were also conducted in a panel of mice infected by lethal *S. aureus* (MRSA), with once daily intragastric (i.g.) administration with 40 mg/kg for 3 consecutive days. The results in Figure 9 show that compound **13u** and valnemulin displayed equivalent *in vivo* potency with 60% survival while **13e** and **13y** provided the infectious mice with 30 and 40% survival, respectively, though **13e** and **13y** exhibited superior

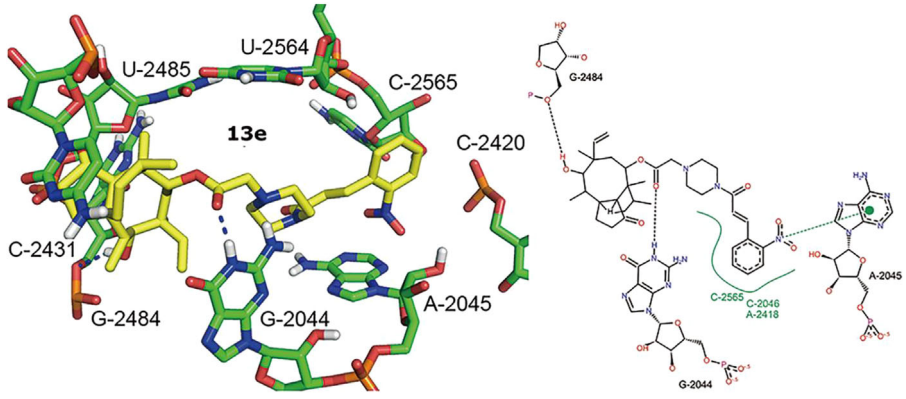

FIGURE 5 Docking mode of **13e** in the active site of the 50S ribosome subunit

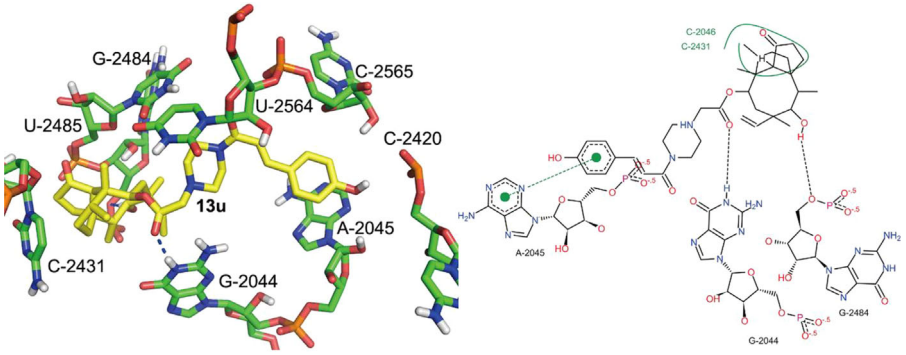

FIGURE 6 Docking mode of **13u** in the active site of the 50S ribosome subunit

effectiveness *in vitro* than both **13u** and valnemulin. The ADME properties as well as the better aqueous solubility and higher melt point of compounds **13u** and valnemulin would explain why they proffered relative better efficacy *in vivo* than that of **13e** and **13y**.

3 | CONCLUSIONS

In summary, a series of novel pleuromutilin derivatives bearing cinnamic acid scaffold and piperazine have been reported. The investigation of these prepared compounds against clinical bacteria demonstrated that most of them owned moderate to good antibacterial activity against Gram-positive bacteria. The SAR study revealed that halogen substitution in the 2-position of cinnamic acid had the same activity as the 3-position and 4-postion regioisomers while compounds with OCH_3 and CH_3 at the 3-position were more active than other two position regioisomers, especially against MSSA and MRSA. Pleuromutilin modifications embracing 2-NO_2 or 4-NO_2 substitutions both exhibited approximate fourfold compared to 3-NO_2 substituted compounds. The MIC values of **13y** were less than that of valnemulin and the excellent *in vivo* potency of **13u** indicates that **13y** and **13u** could be researched deeply in future to find a hit and a promising lead compound for the development of new antibacterial agents.

4 | EXPERIMENTAL

4.1 | Chemistry

The synthesis route and conditions are described in the Supporting Information, which also provides the spectroscopic characterization and the original spectra of the synthesized compounds. The InChI codes of the investigated compounds together with some biological activity data are also provided as Supporting Information.

4.2 | Minimum inhibition concentration testing

The minimum inhibitory concentrations (MICs) of target compounds against bacteria were determined by an agar dilution method in accordance with the methods of the National Committee for Clinical Laboratory Standards (NCCLS) and valnemulin was employed as the positive control. Target compounds were dissolved in 30% aqueous solution of DMSO to prepare stock solutions with an initial concentration of 640 μg/mL. A series of twofold dilutions were prepared from the stock solutions using sterile water followed by a 10-fold dilution with Muller–Hinton (MH) agar medium to provide concentrations ranging from 64 to 0.05 μg/mL. MH broth was employed to culture the tested organisms at 37°C for 12 h, which were detected via OD values to adjust their concentrations to 10^6

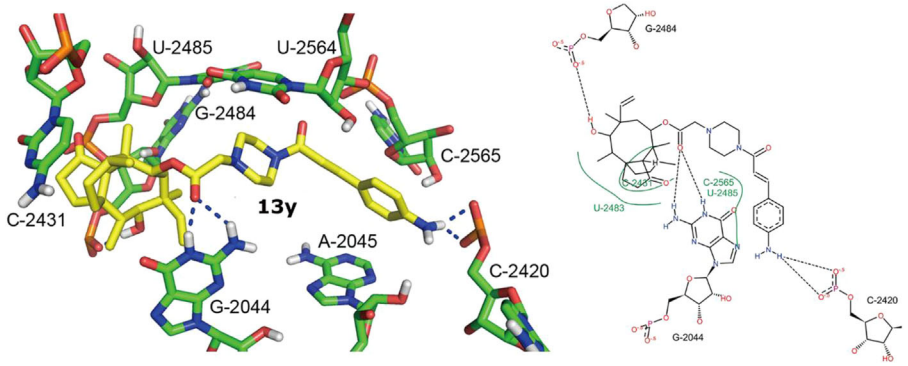

FIGURE 7 Docking mode of **13u** in the active site of the 50S ribosome subunit

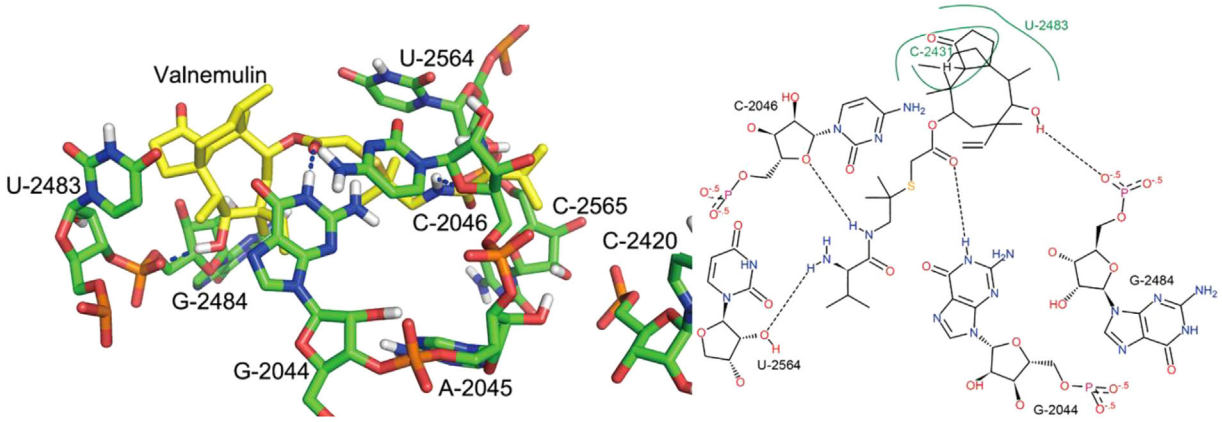

FIGURE 8 Docking mode of valnemulin in the active site of the 50S ribosome subunit

CFU/mL. The bacterial suspensions were inoculated onto the 96-well plates filled with varying concentrations of drugs which were 64, 32, 16, 8, 4, 2, 1, 0.5, 0.25, 0.125 μg/mL from well 1 to well 10 using a multipoint inoculator and incubated at 37°C for 24 h. Each well contained 100 μL bacterial suspension and 100 μL compound solution. Each concentration of testing compounds embraced three parallels for each bacterium.

4.3 | Molecular docking

The energy minimization was performed in the GAFF force field to optimize the docking compounds using AmberTools 14, with the steepest descent method to optimize 2000 steps followed using the conjugate gradient method to optimize 1000 steps furtherly. The AM1-BCC charge was added to the optimized structures and finally stored as a mol2 file for subsequent docking.

AutoDockTools 1.5.6[23] was used to prepare the peptidyl transferase center (PTC) mode based on the crystal structure of *Deinococcus radiodurans* in complex with tiamulin (PDB ID:1XBP).[24] Co-crystallized ligands and crystallographic water molecules were removed. Addition of hydrogens, merger of nonpolar hydrogens to the atom to which they were attached. The PTC model was established comprising residues within a spherical cut of 10 Å around the PTC binding site of 1XBP. Molecular docking was implemented by AutoDock 4.2.6 program.[25] The docking sites were determined according to tiamulin in 1XBP and the specific parameters were listed below: the coordinates of the center point of the interface pocket were (55.425, 124.162, 113.592) and the number of grid points was 60 × 60 × 60 as well as the grid spacing was 0.375 Å. The lattice energy of the interface pocket area was calculated by AutoGrid program. The conformation search strategy adopted the Lamarckian genetic algorithm (LGA) and the key parameters were as follows: number of GA Runs was set to be 100 and the maximum number of evaluations was 25000000, and the rest parameters used default values. PyMOL was employed to achieve docking visualization. The molecular docking results were optimized 1000 steps using the Amber force field in Chimera.

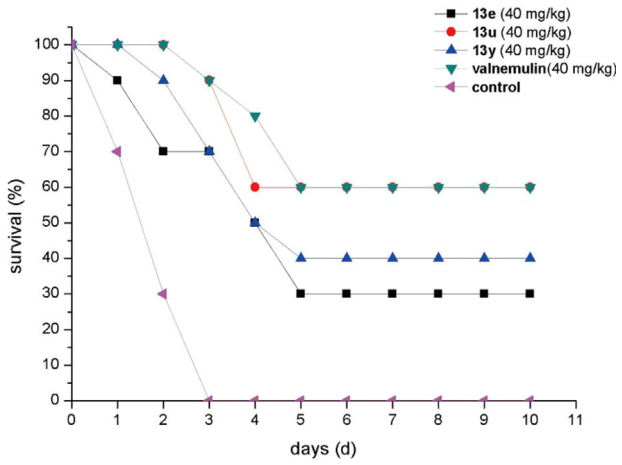

FIGURE 9 Efficacy of compounds **13e**, **13u**, **13y** and valnemulin in the mouse systemic infection model

4.4 | MRSA infection model

4.4.1 Clinical isolate of MRSA

Kunming mice (female, Chongqing Tengxin Bill Experimental Animal Sales Co. Ltd.) weighing 22 ± 2 g were treated with neutropenic for intraperitoneal treatment with 150 mg/kg cyclophosphamide 4 days before infection and with 100 mg/kg 1 day prior to infection. The neutropenic mice were treated with 0.5 mL bacterium suspension via intraperitoneal injection. One hour after infection, the infected mice were conducted intragastric administration with the test compounds **13e**, **13u**, **13y** and valnemulin at doses of 40 mg/kg for 3 consecutive days.The protocol for this study was reviewed and approved by Chongqing Academy of Animal Sciences.

ACKNOWLEDGMENTS

This work was supported by Chongqing Basic Scientific Research Project (No. 16438) and Chongqing Agricultural Development Fund (No. 17412).

CONFLICT OF INTEREST

The authors have declared no conflict of interest.

ORCID

Cheng-hong Li http://orcid.org/0000-0002-5621-4409

REFERENCES

[1] K. K. Kumarasamy, M. A. Toleman, T. R. Walsh, J. Bagaria, F. Butt, R. Balakrishnan, U. Chaudhary, M. Doumith, C. G. Giske, S. Irfan, P. Krishnan, A. V. Kumar, S. Maharjan, S. Mushtaq, T. Noorie, D. L. Paterson, A. Pearson, C. Perry, R. Pike, B. Rao, U. Ray, J. B. Sarma, M. Sharma, E. Sheridan, M. A. Thirunarayan, J. Turton, S. Upadhyay, M. Warner, W. Welfare, D. M. Livermore, N. Woodford, *Lancet Infect. Dis*. **2010**, *10*, 597.

[2] A. Perdih, M. Hrast, K. Pureber, H. Barreteau, S. Gobec, G. Wolber, T. Solmajer, *J. Chem. Inf. Model*. **2014**, *54*, 1451.

[3] A. Perdih, M. Hrast, K. Pureber, H. Barreteau, S. G. Grdadolnik, D. Kocjan, S. Gobec, T. Solmajer, G. Wolber, *J. Comput. Aided Mol. Des*. **2015**, *29*, 541.

[4] W. Kim, W. Zhu, G. L. Hendricks, D. V. Tyne, A. D. Steele, C. E. Keohane, N. Fricke, A. L. Conery, S. Shen, W. Pan, K. Lee, R. Rajamuthiah, B. B. Fuchs, P. M. Vlahovska, W. M. Wuest, M. S. Gilmore, H. Gao, F. M. Ausubel, E. Mylonakis, *Nature* **2018**, *556*, 103.

[5] F. Kavanagh, A. Hervey, W. J. Robbins, *Proc. Natl. Acad. Sci. U. S. A.* **1951**, *37*, 570.

[5] F. Kavanagh, A. Hervey, W. J. Robbins, *Proc. Natl. Acad. Sci. U. S. A.* **1951**, *37*, 570.

[6] S. M. Poulsen, M. Karlsson, L. B. Johansson, B. Vester, *Mol. Microbiol.* **2001**, *41*, 1091.

[7] C. Davidovich, A. Bashan, T. Auerbach-Nevo, R. D. Yaggie, R. R. Gontarek, A. Yonath, *Proc. Natl. Acad. Sci. U. S. A.* **2007**, *104*, 4291.

[8] N. Woodford, M. Afzal-Shah, M. Warner, D. M. Livermore, *J. Antimicrob. Chemother*. **2008**, *62*, 766.

[9] R. Novak, *Ann. N. Y. Acad. Sci*. **2011**, *1241*, 71.

[10] O. Goethe, A. Heuer, X. Ma, Z. Wang, S. B. Herzon, *Nat. Prod. Rep*. **2018**, https://doi.org/10.1039/c8np00042e.

[11] C. Ling, L. Fu, S. Gao, W. Chu, H. Wang, Y. Huang, X. Chen, Y. Yang, *J. Med. Chem*. **2014**, *57*, 4772.

[12] D. A. Williamson, G. P. Carter, B. P. Howden, *Clin. Microbiol. Rev*. **2017**, *30*, 827.

[13] W. T. Prince, Z. Ivezic-Schoenfeld, C. Lell, K. J. Tack, R. Novak, F. Obermayr, G. H. Talbota, *Antimicrob. Agents Chemother*. **2013**, *57*, 2087.

[14] S. Paukner, R. Riedl, *Cold Spring Harb. Perspect. Med*. **2017**, *7*, a027110.

[15] Lefamulin Evaluation Against Pneumonia (LEAP 2) Phase 3 Topline Results, https://investors.nabriva.com/static-files/5c34b447-99cc-4739-b9d6-d4ea4c7d13b9, accessed 2018/10/26.

[16] M. A. Grady, T. L. Gasperoni, P. Kirkpatrick, *Drug Discov*. **2003**, *2*, 427.

[17] J. Heeres, L. J. J. Backx, J. H. Mostmans, J. Van Cutsem, *J. Med. Chem*. **1979**, *22*, 1003.

[18] Y. Wang, W. K. Law, J. S. Hu, H. Q. Lin, T. M. Ip, D. C. C. Wan, *J. Chem. Inf. Model*. **2014**, *54*, 3046.

[19] V. D. De, L. Friggeri, F. D. D'Auria, F. Pandolfi, F. Piccoli, S. Panella, A. T. Palamara, G. Simonetti, L. Scipione, S. R. Di, *Bioorg. Med. Chem. Lett*. **2014**, *24*, 1502.

[20] J. D. Guzman, P. N. Mortazavi, T. Munshi, D. Evangelopoulos, T. D. Mchugh, S. Gibbons, J. Malkinson, S. Bhakta, *MedChemComm* **2014**, *5*, 47.

[21] B. Jayaprakasam, M. Vanisree, Y. Zhang, D. L. Dewitt, M. G. Nair, *J. Agric. Food Chem*. **2006**, *54*, 5375.

[22] D. H. Wei, G. D. Zhao, M. Yu, B. Jiang, *Chin. J. Clin. Pharmacol*. **2016**, *32*, 294.

[23] M. F. Sanner, *J. Mol. Graph. Model*. **1999**, *17*, 57.

[24] F. Schlunzen, E. Pyetan, P. Fucini, A. Yonath, J. M. Harms, *Mol. Microbiol*. **2004**, *54*, 1287.

[25] G. M. Morris, R. Huey, W. Lindstrom, M. F. Sanner, R. K. Belew, D. S. Goodsell, J. Olson Arthur, *J. Comput. Chem*. **2009**, *30*, 2785.

SUPPORTING INFORMATION

Additional supporting information may be found online in the Supporting Information section at the end of the article.

How to cite this article: Deng Y, Tang D, Wang Q-r, Huang S, Fu L-z, Li C-h. Semi-synthesis, antibacterial activity, and molecular docking study of novel pleuromutilin derivatives bearing cinnamic acids moieties. *Arch Pharm Chem Life Sci*. 2018;1–8. https://doi.org/10.1002/ardp.201800266